# SIMULATION OF HIGHLY ELASTIC FLUID FLOWS WITHOUT ADDITIONAL NUMERICAL DIFFUSIVITY

Fernando G. Basombrío

Gustavo C. Buscaglia

Enzo A. Dari

División Mecánica Computacional, DIA

Centro Atómico Bariloche, CNEA

8400 S.C. de Bariloche, RN, Argentina

S.C. de Bariloche, March, 1990

## SUMMARY

A transient decoupled method to treat viscoelastic flows is presented, using Lagrange-Galerkin techniques for velocities and the Lesaint-Raviart method for extra-stresses.

An important point of our scheme is the linear interpolation employed for all fields: This allows for high Weissenberg numbers to be reached with no need for streamline upwinding (SU).

Numerical results for the 4:1 plane contraction are presented, including comparisons with other methods and an example that shows the effect of SU addition.

## 1 - INTRODUCTION

In recent years, important progress has been made in the numerical simulation of viscoelastic fluid flows for increasing elasticities. It has been shown that apparent limits in the Weissenberg (We) or Deborah (De) numbers were mainly due to singularities (turning points, bifurcations, etc.) [1,4,6,13] in the system of discrete equations, and could be overcome by improving the numerical methods. Nevertheless, the High Weissenberg Number Problem remains an open question in computational fluid dynamics (see the review papers in Refs. 10 and 11).

One important step towards extending the range of solvable flows - up to De = 6 (we refer in all cases to the popular 4 : 1 contraction problem) - was given by Marchal and Crochet [7,8] by eliminating spurious wiggles already present in the newtonian limit for many mixed formulations. They required the gradient of discrete velocities to belong to the space of discrete stresses, either exactly [7] or approximately [8], thus allowing their scheme to reduce to the classical UVP formulation when We = 0.

Further improvement came once more from avoiding spurious oscillations: Those arising when conventional Galerkin finite elements are used for hyperbolic equations such as the constitutive law of viscoelastic stresses. In the context of coupled approaches, Marchal and Crochet [8,9] introduced non-consistent streamline upwinding (SU) and carried out the first successful simulation of highly elastic fluids (with no apparent limit in De).

Decoupled techniques are more flexible in what concerns integration of the constitutive equation, and many variants have been published [1-5, etc.]. Nevertheless, only Fortin and Fortin

[3] could increase De without apparent limit, again after adding SU to their original method.

To our knowledge, for the 4:1 contraction problem no simulation has so far been reported for De > 7 without non-consistent streamline dissipation. The effect of this extra-term is however not fully understood, as it surely modifies convergence rates and distorts the underlying set of equations. Moreover, it is quite logical to mistrust the SU method when its consistent counterpart (the well-known SUPG [16]) behaves *as poorly as the classical Galerkin* for the flows under consideration with both coupled [8] and uncoupled [2] schemes.

In this paper, we present a transient decoupled approach capable of handling highly elastic flows *without resource to additional numerical diffusivity*. The finite element method, based upon the Lesaint-Raviart technique, was first used by Fortin and Fortin [3]. Our improvement comes (not surprisingly) from eluding second-order elements, which exhibit oscillatory internal modes. We thus confirm the clever conjecture of Ref.3 about the convenience of low-degree interpolation. In our work we use a piecewise linear continuous approximation for velocities and pressures (Courant triangles). In order to satisfy the LBB condition, each pressure element contains four velocity elements. Viscoelastic stresses are approximated by *piecewise linear and discontinuous triangles, in correspondence with the velocity mesh*. This discretization has good properties of mass conservation, and reduces to the UVP formulation in the Newtonian limit by satisfying the requirement of Marchal and Crochet [7].

In Section 2 of the paper we establish the basic equations of the problem. The numerical method is described in Section 3. Our main results are presented in Section 4, together with comparisons with previous works. Section 5 is devoted to the discussion of results, also studying the effect of SU for high elasticities, and Section 6 to the conclusions.

## 2 - BASIC EQUATIONS

From the constitutive equations

$$T = T_N + \tau \qquad \text{(extra-stress decomposition)} \tag{2.1}$$

$$\tau + \lambda \overset{\square}{\tau} = 2\,\mu_1 \mathbf{d} \qquad \text{(viscoelastic part)} \tag{2.2}$$

$$T_N = 2\,\mu_2\,\mathbf{d} \qquad \text{(newtonian part)} \tag{2.3}$$

for the Cauchy's stress tensor splitting into a spherical part and extra-stress

$$\sigma = -\,p\,\mathbf{1} + T, \tag{2.4}$$

the momentum and mass conservation equations, one gets the final system

$$\rho\,\frac{D\vec{v}}{Dt} - \operatorname{div}\tau - \mu_2 \nabla^2 \vec{v} + \nabla p = \rho \ell \tag{2.5}$$

$$\tau + \lambda \overset{\square}{\tau} = 2\,\mu_1\,\mathbf{d} \tag{2.6}$$

$$\operatorname{div}\vec{v} = 0 \tag{2.7}$$

for the unknown fields of velocity ($\vec{v}$), pressure (p) and viscoelastic extra-stress ($\tau$), with the following notation:

$\frac{D}{Dt}$ : material time derivative

$\overset{\square}{\tau} = \frac{\partial \tau}{\partial t} + \vec{v}\cdot\nabla\tau + \tau.\mathbf{r} - \mathbf{r}.\tau - \theta\,(\mathbf{d}.\tau + \tau.\mathbf{d})$,

$\theta \in [-1,1]$ : objective stress rate

$\rho$ : specific mass

$f$ : body forces

$\nabla$ : the "nabla" operator

$\mathbf{d}$ (resp. $\mathbf{r}$): symmetric (resp. antisymmetric) part of the velocity gradient

$\lambda$ : characteristic time

$\mu_1$, $\mu_2$: polymer and solvent viscosities.

These equations corresponds to a Johnson-Segalman fluid with additional viscosity (fluid of Jeffreys type). For later use, we also introduce the tensor

$$T_A = \tau + \frac{\mu_1}{\lambda} \mathbf{1} \tag{2.8}$$

associated with the well-posedness of the problem when $\mu_2 = 0$ (Maxwell model) [12].

## 3 - DISCRETE FORMULATION

We begin the discretization procedure of (2.5)-(2.7) by decoupling velocity and pressure from extra-stress unknowns, that means

ALGORITHM: For each time step

Step 1: Solve the mass (2.7) and momentum (2.5) balance equations for $\vec{v}^{\,n+1}$ and $p^{n+1}$ keeping $\tau^n$ fixed.

Step 2: Solve the viscoelastic constitutive equation (2.6) for $\tau^{n+1}$ keeping $\vec{v}^{\,n+1}$ fixed

Step 3: Check for convergence (if searching a steady-state solution) and go back to Step 1 if necessary.

This algorithm has already been successfully used by Fortin and Fortin [3]. Step 1 amounts to the solution of a transient Navier-Stokes problem, which we compute by means of the direct Lagrange-Galerkin (characteristics) method [14] with non-exact integration at the mid-sides of each (triangular) element.

Preconditioned conjugate gradients [15] are then used to solve the resulting system of equations.

Step 2 requires the solution of a linear hyperbolic system, and the Lesaint-Raviart method is used to handle it at element level. Convergence was checked by evaluating the relative variation of solutions in the maximum norm. Although none of these techniques is innovative, let us briefly outline the discrete equations of Step 2.

After (implicit) temporal discretization (of time step $\Delta t$), equation (2.6) can be written in compact form as

$$\lambda\, \vec{v}\,.\,\nabla\, \tau^{n+1} + L\, \tau^{n+1} = \mathbf{F} \tag{3.1}$$

where L denotes the linear operator

$$L\tau^{n+1} = \left[1 + \frac{\lambda}{\Delta t}\right]\tau^{n+1} + \lambda\left[\tau^{n+1}.\,\mathbf{r} - \mathbf{r}.\,\tau^{n+1} - \theta\left(\mathbf{d}.\,\tau^{n+1} + \tau^{n+1}.\,\mathbf{d}\right)\right] \tag{3.2}$$

and

$$\mathbf{F} = 2\,\mu_1\,\mathbf{d} + \frac{\lambda}{\Delta t}\,\tau^{n} \tag{3.3}$$

Introducing now the finite element space

$$W_h = \left\{ w \in L_2(\Omega),\ w|_K \in P_k\,(K),\ \forall\, K \in \mathcal{T}_h \right\} \tag{3.4}$$

of piecewise polynomials in a triangulation $\mathcal{T}_h$ of the domain $\Omega$, with no continuity requirements at interelement boundaries, the Lesaint-Raviart method [17] for the viscoelastic constitutive equation reads

$$\sum_{K\in\mathcal{T}_h} \left\{ \int_K \left(\lambda\vec{v}.\,\nabla\tau_h^{n+1} + L\,\tau_h^{n+1}\right) :\ \chi\ dx\ + \right.$$

$$+ \int_{\partial K_-} \lambda \left[\tau_e^{n+1} - \tau_i^{n+1}\right] : \chi_i \ \vec{v}.\vec{n} \ d\Gamma \Big\} =$$

$$= \int_{\Omega} F : \chi \ dx \qquad \forall \ \chi \in (W_h)^{n \times n}_{s} \qquad (3.5)$$

where $\partial K_-$ stands for the inflow boundary of element K, and subscript "e" (resp. "i") represents the external (resp. internal) evaluation of the function at $\partial K_-$. $(W_h)^{n \times n}_{s}$ is the space of symmetric tensor fields with components in $W_h$.

It should be kept in mind that a certain amount of upwinding is automatically introduced by the previous formulation. Error bounds of order $h^{k+\frac{1}{2}}$ are shown in Ref.25.

Equation (3.5) can be solved at element level, provided $\tau_e^{n+1}$ is known whenever needed. This requires a flow-dependent ordering of the mesh elements, starting at $\partial\Omega_-$ (inflow boundary). Nevertheless, except for uniform velocity fields, such an optimal ordering fails to exist in the general case, as can be readily seen in the example of Fig.1. We successfully avoided this obstacle by successive relaxation *together with* the following strategy (repeated at each time step), which we give in detail:

- Compute the upstream neighbours for all elements.
- Order first all elements that need no iterative solution, starting at $\partial\Omega_-$ (that is, until situations analog to that of Figure 2 arise, and no element exists whose upstream neighbours have already been numbered). These conform a connected (if $\partial\Omega_-$ is connected) set of elements that we will call "independent sub-mesh".
- Starting at the boundary of the independent sub-mesh, let the ordering front go ahead including that element that receives flow from not-already-numbered neighbours *through*

*less than a half side*. Such an element generally exists for triangles if the flow is approximately incompressible (if this is not the case, it is always possible to arbitrarily choose an element adjacent to the ordering front and continue).

- Once all elements have been numbered, sweep the independent sub-mesh solving (3.5).
- Finally, with initial guess $\tau_h^n$, sweep the remaining elements in the prescribed order, as many times as required for convergence.

This relaxation procedure based upon flow-oriented ordering required in most time steps only *two* iterations to converge within a tolerance (in the maximum norm) of $10^{-5}$.

It is also possible to introduce in (3.5) a non-consistent streamline upwinding by adding an anisotropic diffusivity proportional to local mesh size in the flow direction. This was implemented to allow for comparison with the pure Lesaint-Raviart method.

## 4 - NUMERICAL RESULTS

These concern the well-known benchmark of the planar four-to-one contraction (see layout with dimensions and boundary conditions in Fig.2), for the upper-convected case ($\theta = 1$), with solvent viscosity $\mu_2 = 0.11$ and viscosity ratio

$$\frac{\mu_2}{\mu_1 + \mu_2} = 0.11 \tag{4.1}$$

The Deborah number is defined as

$$De = \lambda \, \dot{\gamma}_w \tag{4.2}$$

where $\dot{\gamma}_w$ is the shear-rate at the downstream distant wall.

The finite element mesh is also shown in Fig.2 (post processing was made with program PITUCO [19]), it consists of 1868 velocity-stress elements, with a total of 19139 unknowns. Care was taken to avoid abrupt mesh size changes, which could probably generate spurious oscillations in the stress field [3].

We used the transient method of Section 3 to obtain steady-state solutions. In fact, we began with the newtonian case and slowly stepped the Deborah number towards higher elasticities (the typical step was 1). To do this, we followed two alternatives:

- To use the latest results as initial condition, or,
- To perform a *linear* extrapolation of *all fields* from the latest two De, and use this rough guess as initial state for a new (with higher $\lambda$) calculation.

The latter approach turned out to be economically preferable, as convergence was attained faster.

With a time step of 0.02, we were able to reach De = 18. In Figure 3 the velocity on the symmetry axis is plotted for various De. As elasticity is increased, the streamlines move left in the vicinity of the contraction, thus reducing the shear rate at the wall. A macroscopic effect of this phenomenon is the Couette correction, given by

$$C = \frac{\Delta p - \Delta p_{fd}}{2\, \tau_w} \qquad (4.3)$$

where $\Delta p$ stands for the calculated pressure difference, $\Delta p_{fd}$ for that obtained assuming fully developed flow in both channels which conform the contraction problem, and $\tau_w$ represents the fully developed wall shear stress in the downstream section. In Figure 4 we show C values obtained by the present method (program FVELR).

To allow for comparison, we also include results from Debbaut, Marchal and Crochet [9], and from a simultaneous calculation by a method of characteristics developed by Basombrío [5] (program FVE4). For high elasticities our results are probably inaccurate due to inadequate exit channel length, as discussed in Ref.9. The matching of all predictions is nevertheless satisfactory.

Let us now concentrate on the normal 2-2 component of the viscoelastic stress near the contraction. This field exhibits a sharp peak at the re-entrant corner which seems to be the source of excessive numerical errors and consequent loss of stability for most of the available methods. In fact, the algorithm of characteristics of Basombrío [5], using quadratic interpolation, failed to converge for De > 6.07, and the break-out symptom was the severe local distortion of all fields at or near the re-entrant corner. It is then interesting to compare the $\tau_{22}$ fields along the vertical line through the singularity obtained with the present method (FVELR) and that of Ref.5 (FVE4) at De = 6. This is shown in Figure 5a, where oscillations behind the peak are much less pronounced for FVELR.

Other comparisons with results obtained with the program FVE4 [5] are shown in Figs.5b and 6.

Although our results of Fig.5a are not as smooth as we would have desired, we found no convergence limit in the Deborah number (see discussion in Section 5). After reaching De = 18, it became obvious that a new (longer) geometry was required to continue. We prefered to leave this for future work and turn to another crucial aspect of viscoelastic flow simulation: The influence of adding SU dissipation to the discrete formulation (3.5). The vertical velocity along $x_1 = 0$ and the $\tau_{22}$ stress along $x_2 = 1$, with and without SU, are presented in Figures 7 and 8 for De = 18. We also observed an *enlargement* of the corner vortex after SU addition (see streamlines in Fig.9), together with a significant rise in the total pressure loss (see Fig.4).

All the described results were run on a VAX11/780 computer.

## 5 - DISCUSSION

Some topics in the previous results deserve additional comment. To assess the numerical accuracy of the method, a condition number may be defined as

$$q = 2 \left( \frac{s_2}{s_1} + \frac{s_1}{s_2} \right)^{-1} \tag{5.1}$$

where $s_1$ and $s_2$ are the two non-trivial eigenvalues of $T_A$. It can be shown [12] that q must remain positive throughout the domain if proper initial and boundary conditions are imposed. In Figure 10, we plot the number of nodes with negative q as a function of De for the obtained steady-states. Clearly, the solution progressively gets ruined with increasing elasticity, and covergence difficulties are to be expected at some higher De [6] (i.e., a limit point probably exists, although not reached). Nodes with $q < 0$ appear in the downstream neighbourhood of the singularity. This is partially corrected after SU addition (Fig.10), but with great distortion of all fields (see Fig.4, 7, 8 and 9), at least for our mesh and element,. Note that the peak stress value becomes *larger* with SU, contrary to expectation, but the dynamic effect decreases due to lower stress gradients.

The comparison of Fig.5a shows one of the advantages of linear elements. The quadratic interpolation of FVE4 [5] allows for spurious osillations inside each element that locally pollute the stress field. This effect was also observed by Fortin and

Fortin [3], and our results confirm their assumption that linear elements could be an improvement.

While tunning parameters (particularly the time step) for the results of Section 4, we did observe some instabilities together with loss of convergence of the algorithm. One of the advantages of our transient approach is that such phenomena can be traced back and partially understood. Our experiences revealed that instabilities arise in regions with strong coupling of unknowns, where an unstable distortion of the velocity field develops during the iterative process. By unstable we mean that such a distortion modifies the stresses towards its own amplification and collapse. This happens *locally* near singularities, while most of the flow seems to be converging. It is not obvious how to control and/or take advantage of this feature to extend convergence limits.

## 6 - CONCLUSIONS

A modified version of the method of Fortin and Fortin [3] has been introduced with linear triangular elements for all fields. In general lines, both the algorithm and the treatment of the constitutive equation remain the same, but the new interpolants bring significant improvement. Indeed, we computed flows up to De = 18 with the pure Lesaint-Raviart method for stresses, while previous schemes need streamline dissipation to go beyond 7.

Once more, our experiences confirm that convergence limits for the High Weissenberg Number Problem can be extended by an appropriate treatment of the hyperbolic character of the constitutive equation. In particular, any effort to avoid spurious oscillations produces better behaviour of the algorithms.

In what concerns the method presented here, some work remains to be done. Extension to more realistic (fully non-linear) differential models is straightforward, and would be useful in applications. From the numerical viewpoint, we have not yet checked convergence with respect to mesh refinement, and the effect of SU addition is still poorly understood.

Acknowledgements.

F.G. Basombrio wishes to express his gratitude to Prof. Roland Glowinski, for his kind invitation to visit the Dept. of Mathematics of the University of Houston and for the fruitful discussions on numerical simulation of viscoelastic fluid flows.

Figure Captions

Fig. 1: Example showing the need for a relaxation scheme. $T|_{K2}$ must be known to find $T|_{K1}$, and viceversa.

Fig. 2: Sketch of the domain and boundary conditions for the 4:1 sudden contraction problem. The finite element mesh used through the calculations is also included.

Fig. 3: Vertical velocity along the symmetry axis as obtained with the present method (——: De = 0, ...: De = 6, ---: De = 12, -.-.-: De = 18).

Fig. 4: A comparison of couette correction prediction for various methods (——: FVELR, ---: FVE4 [5], ...: Debbaut, Marchal and Crochet [9]). ∇ corresponds to FVELR after SU addition.

Fig. 5: a) $\tau_{22}$ viscoelastic stress along the line $x_1 = 1$ at De = 6 (——: FVELR, ...: FVE4 [5]. b) Velocity an the symmetry axis (——: FVELR, ...: FVE4 [5]).

Fig. 6: Streamlines obtained at De = 6 from the program FVE4 (left) and FVELR (right).

Fig. 7: Effect of SU addition on the vertical velocity along $\chi_1 = 0$ for the present method at De = 18 (——: without SU, ...: with SU).

Fig. 8: Effect of SU addition on $\tau_{22}$ profile along $\chi_1 = 1$, for the present method at De = 18 (——: without SU, ...: with SU).

Fig. 9: Streamlines pattern at De = 18 (left: without SU, right: with SU).

Fig. 10: Number of nodes with negative condition number ($q < 0$) as a function of the Deborah number for the present method (——). ∇ corresponds to adding SU diffusivity.

## References


[1] M. Fortin and D. Esselaoui, Int. J. for Num. Meth. in Fluids 7 (1987), 1035.

[2] X.-L. Luo and R.I. Tanner, J.Non Newtonian Fluid Mech. 31 (1989), 143.

[3] M. Fortin and A. Fortin, J.Non Newtonian Fluid Mech. 32 (1989), 295.

[4] M. El Hadj and P.A. Tanguy, "A finite element procedure coupled with the method of characteristics for simulation of the viscoelastic fluid flows". Univ.Laval, Québec. Submitted for publication (1989).

[5] F.G. Basombrío, "Transient flows of viscoelastic fluids treated by the method of characteristics". Submitted for publication (1989).

[6] F. Dupret, J.M. Marchal and M.J. Crochet, J.Non Newtonian Fluid Mech. 18 (1985), 173.

[7] J.M. Marchal and M.J. Crochet, J.Non Newtonian Fluid Mech. 20 (1986), 187.

[8] J.M. Marchal and M.J. Crochet, J.Non Newtonian Fluid Mech. 26 (1987), 77.

[9] B. Debbaut, J.M. Marchal and M.J. Crochet, J.Non Newtonian Fluid Mech. 29 (1988), 119.

[10] R. Keunings, "Simulation of Viscoelastic Fluid Flows", in Fundamentals of Computer Modelling for Polymer Processing, C.L. Tucker III (Ed.), Carl Hauser Verlag, 1987.

[11] M.J. Crochet, Rubber Chemistry and Technology 62 (1989), 426.

[12] F. Dupret and J.M. Marchal, J. Mécanique Théorique et Appliqueé 5 (1986), 403.

[13] F. Dupret and J.M. Marchal, J. Non Newtonian Fluid Mech. 20 (1986), 143.

[14] K.W. Morton, A. Priestley and E. Süli, Math. Modell. and Numer. Anal. 22 (1988), 625.

[15] J. Cahouet and J.P. Chabard, Int.J. Num. Meth. in Fluids 8 (1988), 869.

[16] T.J.R. Hughes and A. Brooks, "A multidimensional upwind scheme with no crosswind diffusion", in T.J.R. Hughes (Ed.), "Finite Element Methods for Convection Dominated Flows", AMD-Vol.34, ASME, New York, (1979), 19-35.

[17] P.Lesaint and P.A. Raviart, "On a finite element method for solving the neutron transport equation", in Mathematical Aspects of Finite Element Methods in Partial Differential Equations, C. de Boor (Ed.), Academic Press, New York, (1974), 89-123.

[18] C. Johnson, U. Nävert and J. Pitkäranta, Comp. Meth. Appl. Mech. Engng. 45 (1984), 285.

[19] M.J. Vénere, Proc. MECOM'88, IX Latinoamerican and Iberic Congress on Computational Methods for Engineering, Córdoba, Argentina, November 1988.

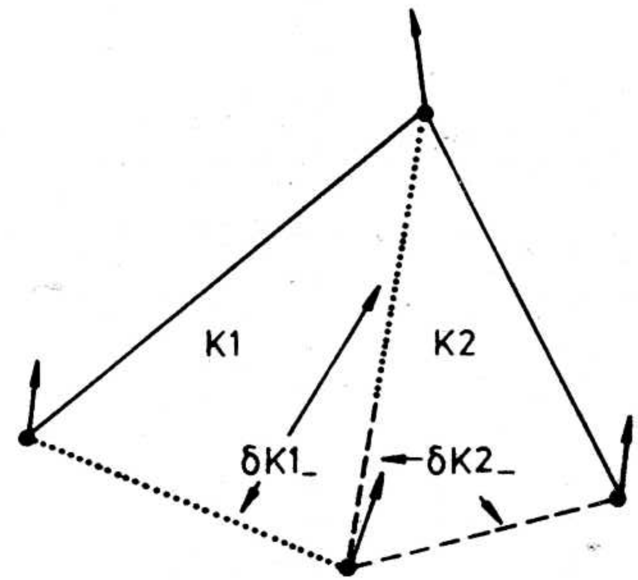


Figure 1

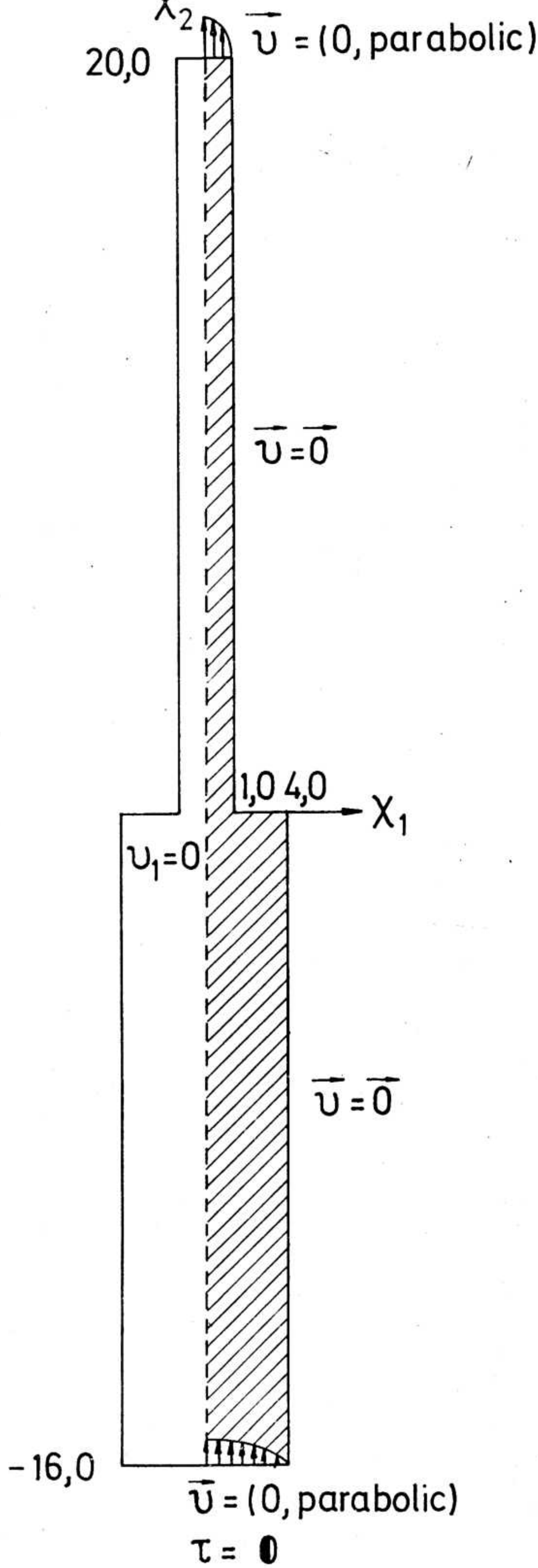

$X_2$
$\vec{v}$ = (0, parabolic)
20,0
$\vec{v} = \vec{0}$
1,0 4,0
$X_1$
$v_1 = 0$
$\vec{v} = \vec{0}$
-16,0
$\vec{v}$ = (0, parabolic)
$\tau = 0$

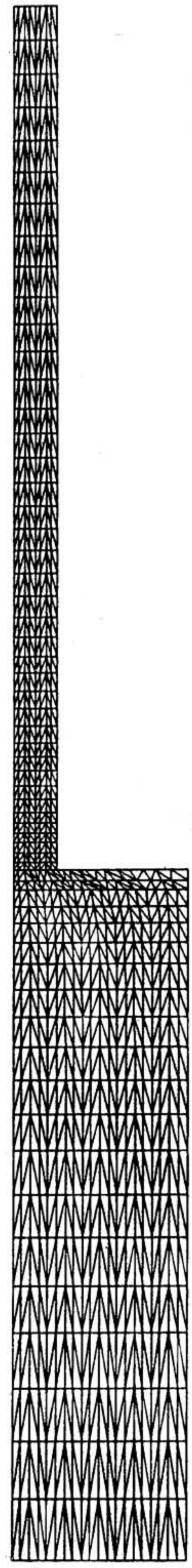

Figure 2

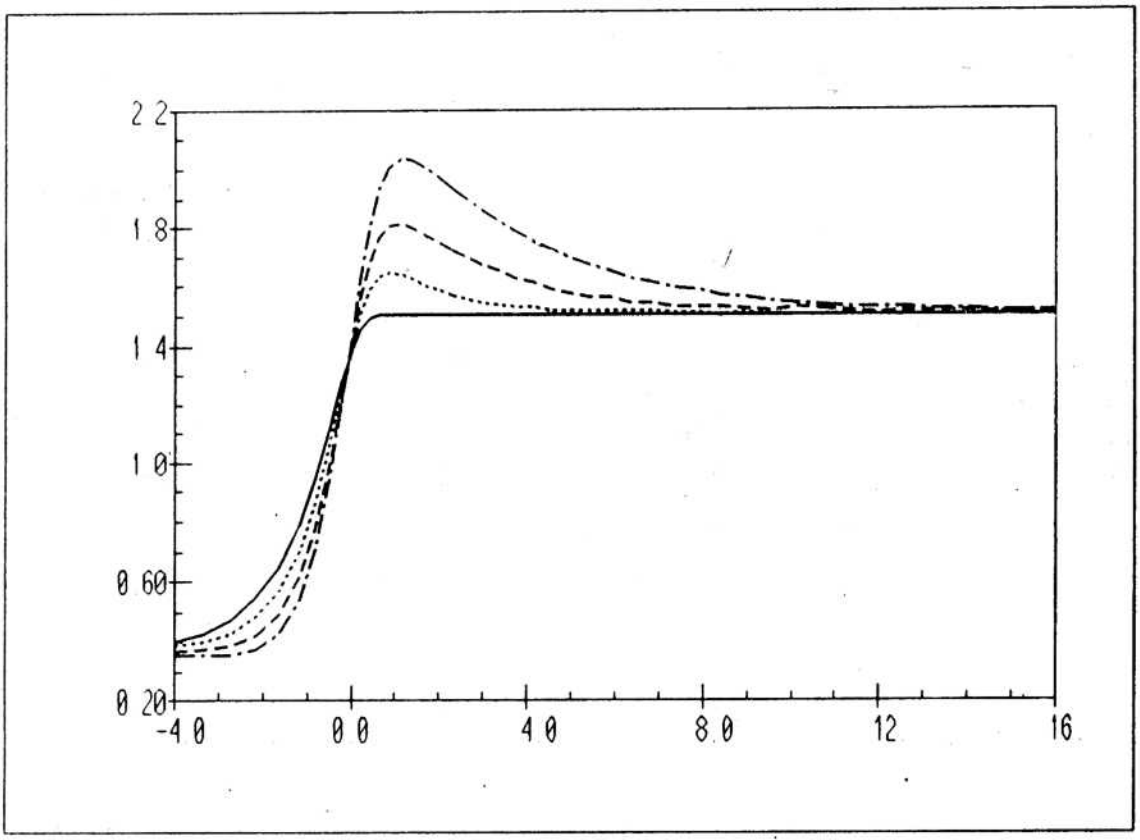


Figure 3

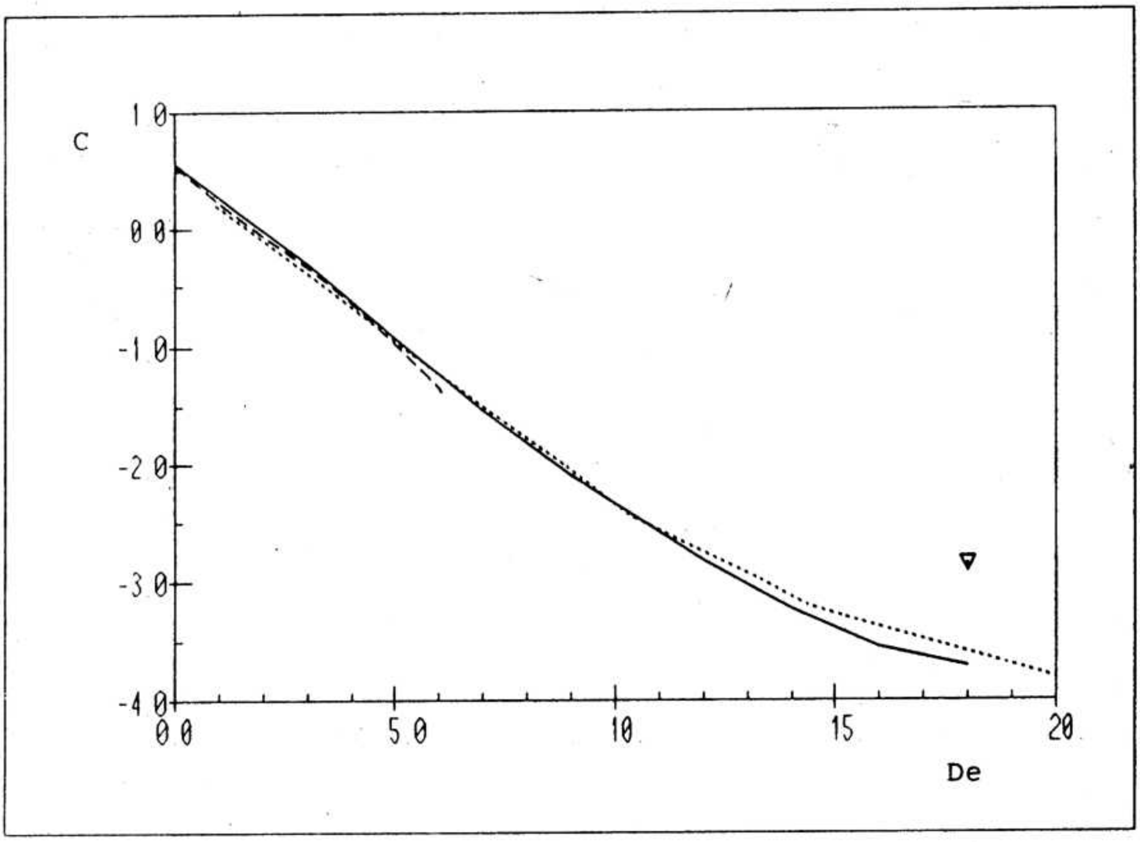


**Figure 4**

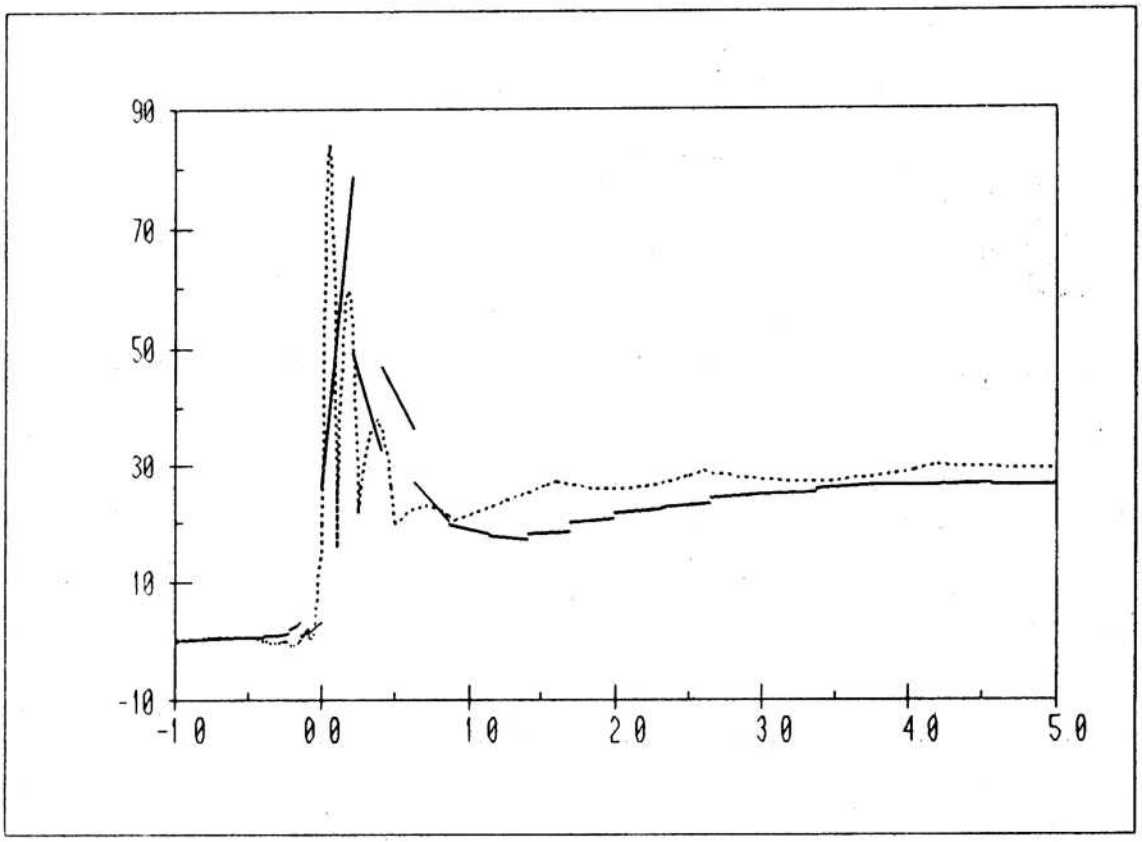


**Figura 5.a**

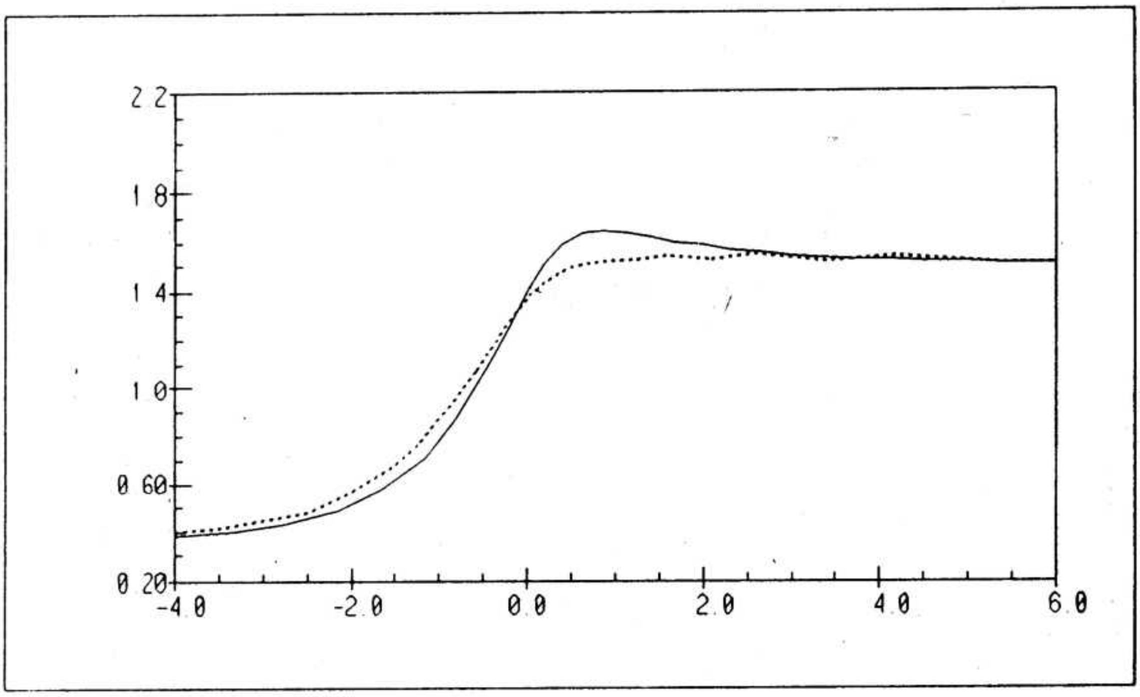


**Figure 5.b**

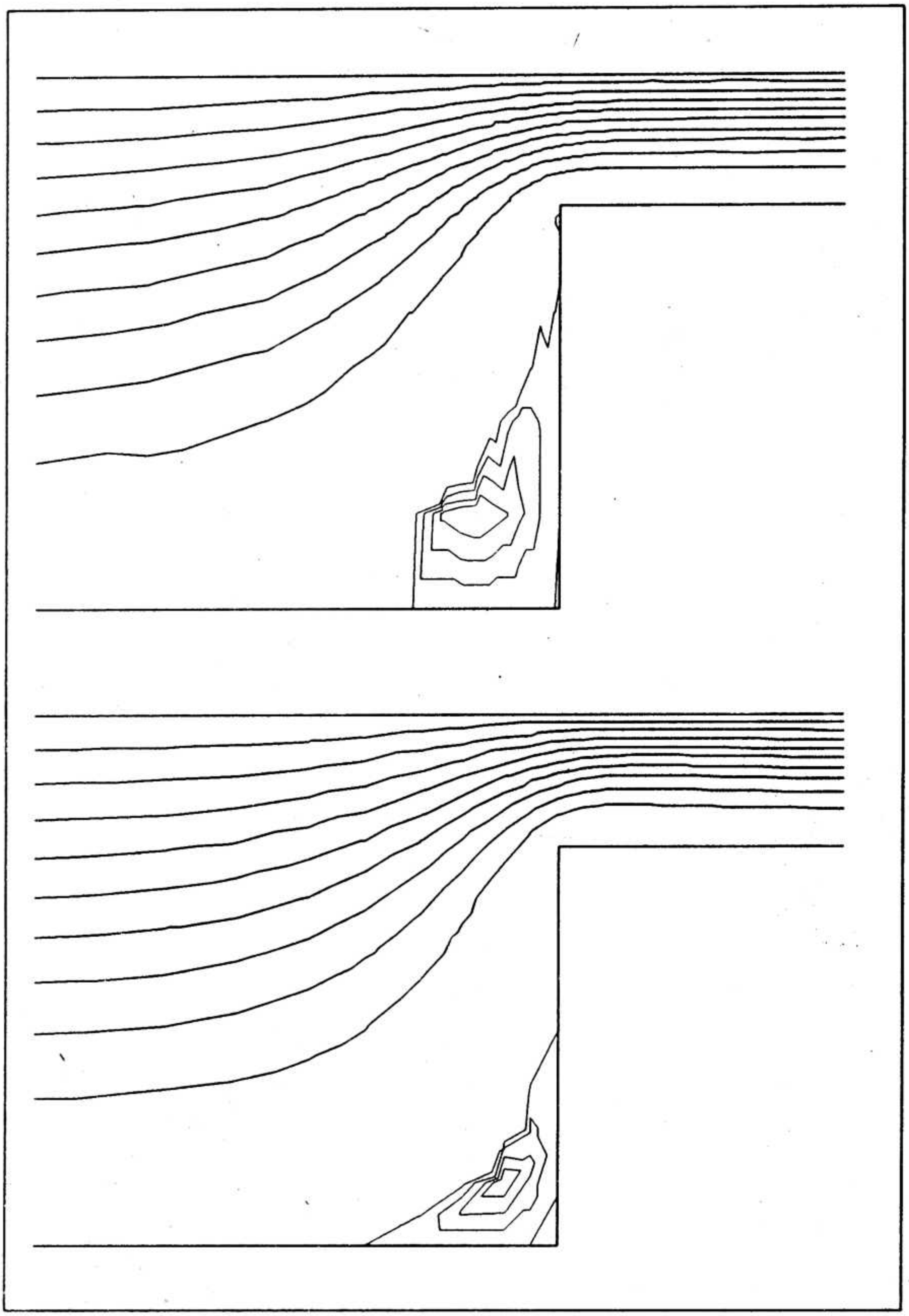

Figure 6

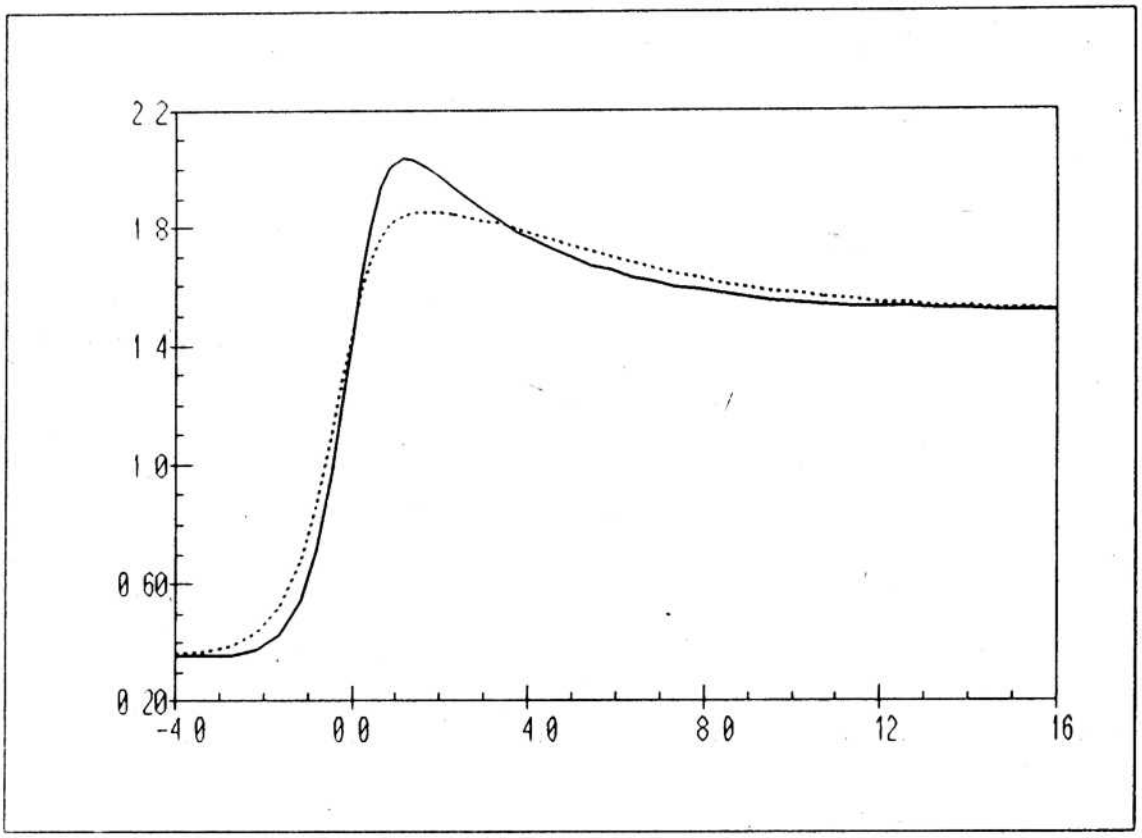


**Figure 7**

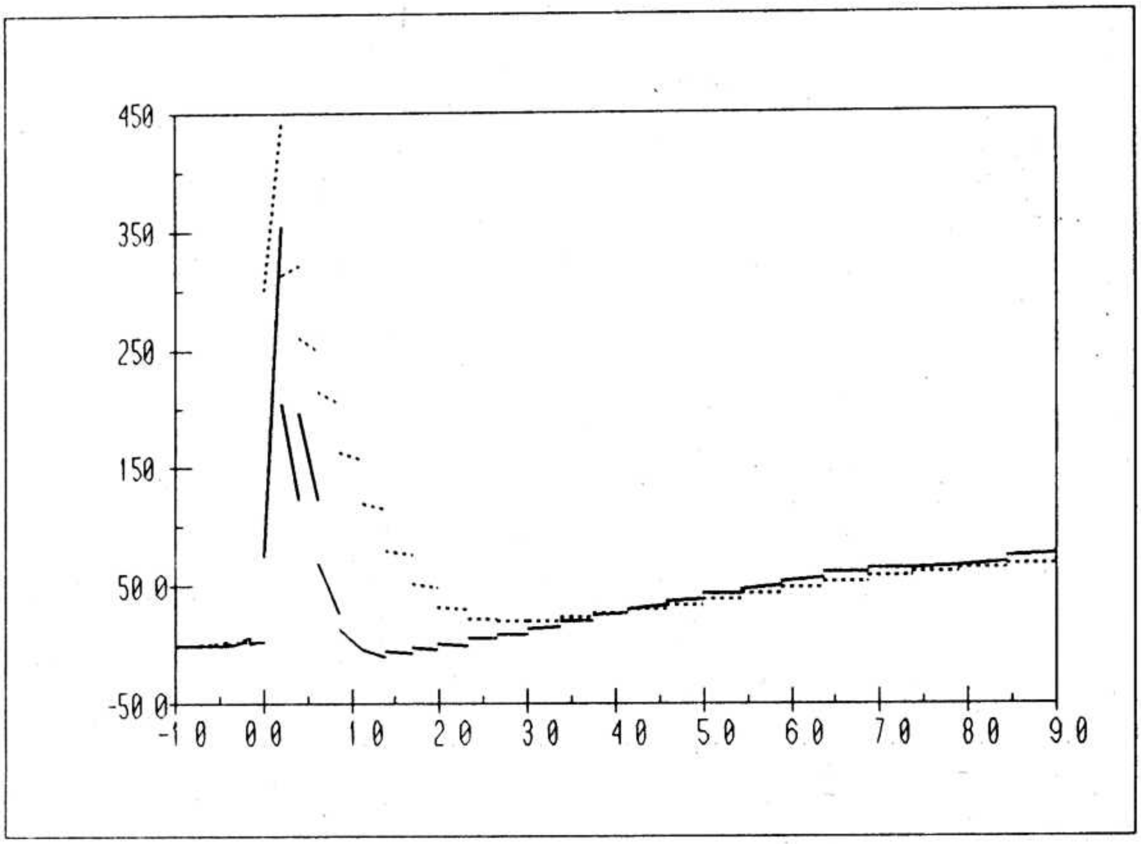


**Figure 8**

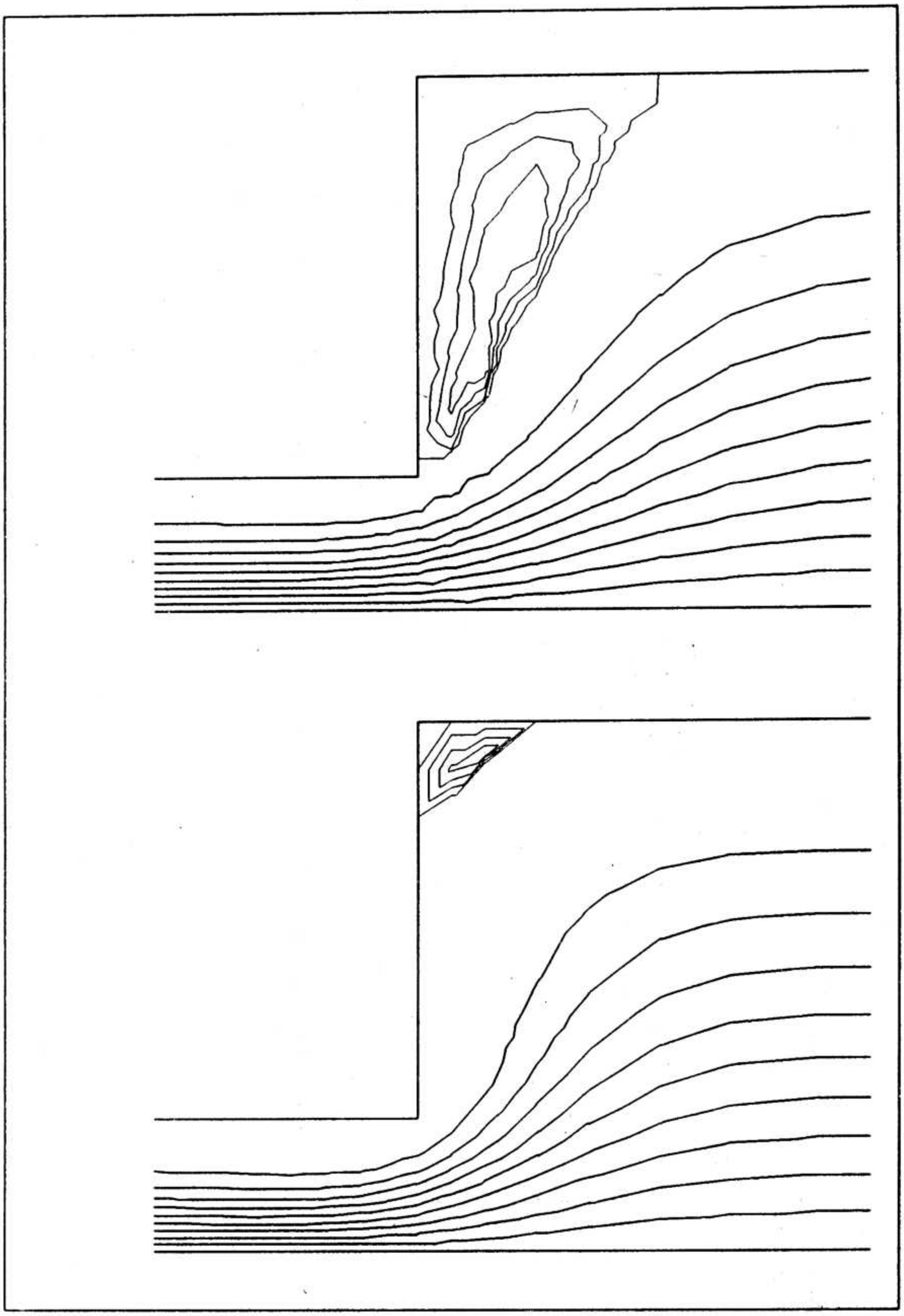

Figure 9

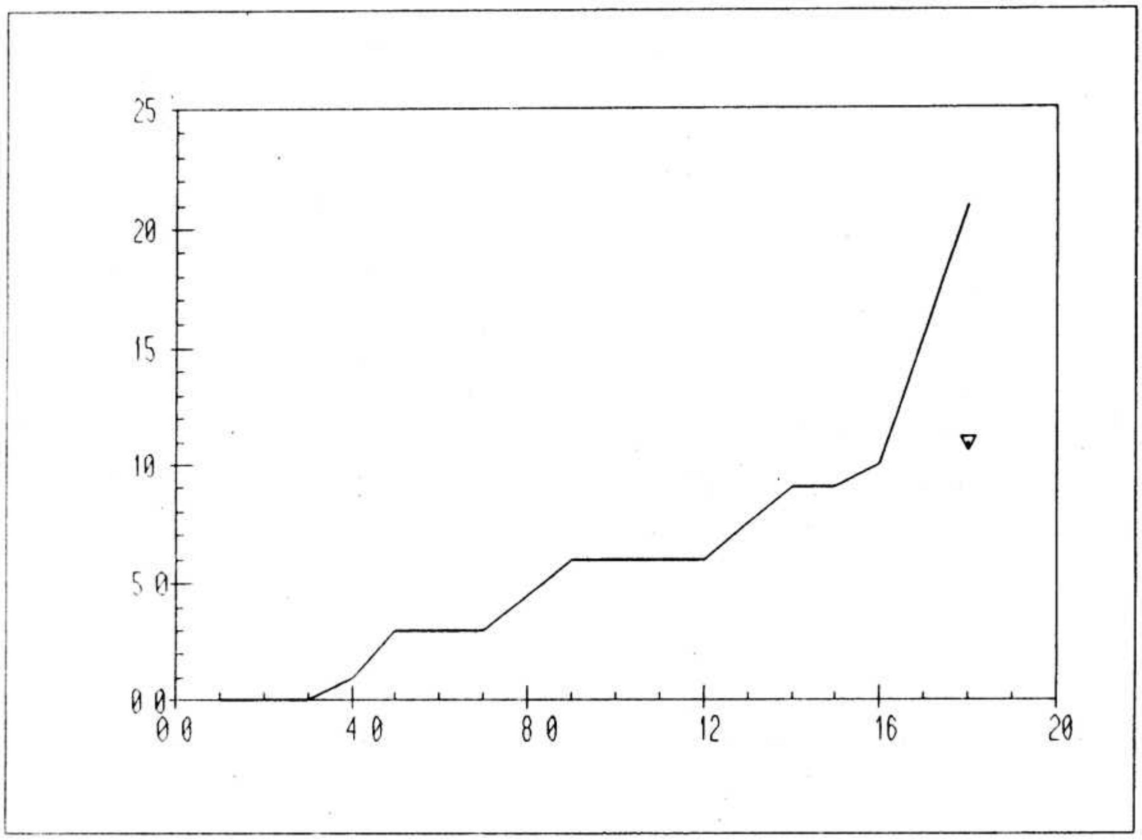


Figure 10